Supported Catalysts

Deutsche Ausgabe: DOI: 10.1002/ange.201507368
Internationale Ausgabe: DOI: 10.1002/anie.201507368

An Atomic-Scale View of CO and H_2 Oxidation on a Pt/Fe_3O_4 Model Catalyst

*Roland Bliem, Jessi van der Hoeven, Adam Zavodny, Oscar Gamba, Jiri Pavelec, Petra E. de Jongh, Michael Schmid, Ulrike Diebold, and Gareth S. Parkinson**

Abstract: *Metal–support interactions are frequently invoked to explain the enhanced catalytic activity of metal nanoparticles dispersed over reducible metal oxide supports, yet the atomic-scale mechanisms are rarely known. In this report, scanning tunneling microscopy was used to study a $Pt_{1\text{-}6}/Fe_3O_4$ model catalyst exposed to CO, H_2, O_2, and mixtures thereof at 550 K. CO extracts lattice oxygen atoms at the cluster perimeter to form CO_2, creating large holes in the metal oxide surface. H_2 and O_2 dissociate on the metal clusters and spill over onto the support. The former creates surface hydroxy groups, which react with the support, ultimately leading to the desorption of water, while oxygen atoms react with Fe from the bulk to create new $Fe_3O_4(001)$ islands. The presence of the Pt is crucial because it catalyzes reactions that already occur on the bare iron oxide surface, but only at higher temperatures.*

Variations in the CO oxidation activity of nominally similar metal nanoparticles dispersed over different metal oxides[1] are a clear indicator of metal–support interactions, but the mechanisms of how the metal oxide gets involved are difficult to ascertain. The support is known to transfer electrons to (or from) the clusters,[2] modifying their shape and adsorption properties, and adsorb reactants and promoters (e.g., water) that can speed up the reaction.[3] At elevated temperature, the so-called Mars–van Krevelen (MvK) mechanism[1i] can operate, where CO molecules extract lattice oxygen atoms ($O_{lattice}$) at the cluster perimeter forming CO_2, and gas-phase O_2 repairs the surface to complete the catalytic cycle. Although there is mounting evidence that the MvK mechanism plays a role when reducible metal oxides are utilized as the support,[1i] there is little atomic-scale information available to better understand how these processes occur.

Herein, we used scanning tunneling microscopy (STM) to follow the evolution of a $Pt/Fe_3O_4(001)$ model catalyst exposed to CO, O_2, and H_2 at 550 K. Holes and islands in the vicinity of Pt clusters provide direct evidence of the reduction and oxidation of the metal oxide in CO- and O_2-rich atmospheres, respectively, while dissociation and spillover of H_2 lead to hydroxylation of the support lattice. We interpret our results as the metal catalyzing reactions that otherwise occur only between the reactants and the support at higher temperatures.

An STM image of the $Pt/Fe_3O_4(001)$ model catalyst utilized as the basis for this work is shown in Figure 1. The $Fe_3O_4(001)$ support[4] exhibits large, flat terraces (Figure 1, inset) characterized by rows of protrusions in STM images related to surface Fe atoms. The rows rotate by 90° from terrace to terrace, which is a consequence of the spinel structure. Surface O atoms are not imaged because they have no density of states in the vicinity of the Fermi energy.[5] Surface OH groups, formed through the reaction of water and oxygen vacancies during sample preparation,[6] modify the density of states of the neighboring Fe atoms, making them

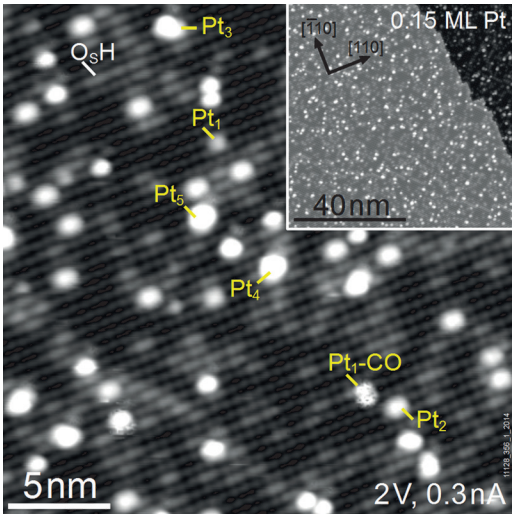

Figure 1. The $Pt_{1\text{-}6}/Fe_3O_4(001)$ model catalyst. The $Fe_3O_4(001)$ support exhibits rows of protrusions related to surface iron atoms. Elongated protrusions on the Fe rows are surface OH groups. $Pt_{1\text{-}6}$ clusters (large, oval protrusions) are formed by exposing 2.7×10^{17} m^{-2} Pt_1 adatoms to CO (1×10^{-7} mbar) for 10 min at room temperature. Upon CO adsorption, otherwise stationary Pt_1 adatoms become mobile and agglomerate. The Pt cluster sizes were assigned on the basis of STM movies in which the agglomeration was tracked atom-by-atom. Inset: On a large scale, the support exhibits large, flat terraces on which the metal particles are randomly distributed.

[*] R. Bliem, O. Gamba, J. Pavelec, Prof. M. Schmid, Prof. U. Diebold, Prof. G. S. Parkinson
Institute for Applied Physics, TU Wien
Wiedner Hauptstrasse 8-10, 1050 Wien (Austria)
E-mail: Parkinson@iap.tuwien.ac.at
J. van der Hoeven, Prof. P. E. de Jongh
Debye Institute for Nanomaterials, Utrecht University
P.O. Box 80.000, 3508 TA Utrecht (The Netherlands)
A. Zavodny
Institute of Physical Engineering, Brno University of Technology
61669 Brno (Czech Republic)
and
CEITEC BUT, Brno University of Technology
61669 Brno (Czech Republic)

Supporting information for this article is available on the WWW under http://dx.doi.org/10.1002/anie.201507368.

appear brighter in STM images.[7] The surface exhibits a ($\sqrt{2}\times\sqrt{2}$)R45° reconstruction,[4] which binds metal adatoms in one particular site per unit cell at temperatures as high as 700 K.[4,8] In this work, randomly distributed Pt clusters with sizes in the range of one to six atoms (Figure 1 a) were prepared by CO-induced sintering of 2.7×10^{17} Pt adatoms per m^2, as demonstrated previously for Pd.[8f] X-ray photoelectron spectroscopy (XPS) measurements (see the Supporting Information, Figure S3) revealed that the CO remained on the clusters, but desorbed when the sample was heated to 550 K.

Exposing the $Pt_{1\text{-}6}/Fe_3O_4$ system to CO, O_2, and H_2 at room temperature resulted in no discernible difference in STM (Figure S2). However, exposure to the same gases at 550 K induced significant modification of the support morphology in the vicinity of the clusters. Following CO exposure, (Figure 2 a, $p_{CO}=1\times10^{-7}$ mbar, 60 min) large holes covering 3.7 % of the surface were observed in the $Fe_3O_4(001)$ terrace. The step height (2 Å) is consistent with the distance between the Fe_{oct}–O planes, and the rows (rotated by 90°) of the underlying Fe_{oct}–O layer are clearly visible inside the larger holes (inset). Each hole is associated with (at least) one Pt cluster, which typically sits at the step edge, but only half of the clusters are associated with holes. Holes were also created when the model catalyst was exposed to H_2 (Figure 2 b, $p_{H_2}=1\times10^{-7}$ mbar, 20 min), but now most clusters appeared inside the holes that cover 8.7 % of the surface. As this occurred in just 20 min, the process is clearly more efficient with H_2. Some redispersion results in the observation of isolated Pt_1 adatoms on the surface.

None of the morphological changes described above occur in the absence of Pt (see Figure S2), but CO and H_2 reduce iron oxides at higher temperatures, producing CO_2 and water, respectively.[9] In the case of CO, the Pt cluster efficiently adsorbs the molecule and delivers it to the cluster–support interface where it extracts $O_{lattice}$ atoms to create CO_2. As some clusters are associated with the removal of many tens of $O_{lattice}$ atoms, while others remain on the pristine substrate, extraction of the first $O_{lattice}$ atom most likely presents a significant energetic barrier. This is in line with recent DFT + U calculations for $CeO_2(111)$, where undercoordinated O atoms at step edges were found to be more easily removed by CO than terrace oxygen atoms.[10] As the clusters are mostly found on the upper step edge of large holes, they most likely diffuse along the step once a hole is nucleated, extracting more and more lattice oxygen atoms as they go. An interesting question remains: Why are holes observed instead of isolated point defects? The answer is that undercoordinated Fe atoms created by the surface reduction diffuse into the bulk, forming interstitials at elevated temperature, as observed previously.[8e,g,11] Oxygen vacancies are not common defects in iron oxides, which handle stoichiometry variation via the cation sublattice.[11]

With H_2, dissociation on the clusters followed by spillover creates surface OH groups, which are known to react with $O_{lattice}$ atoms, leading to the desorption of water above 500 K.[6,12] As OH groups can diffuse over the metal oxide surface at 550 K,[6,12] $O_{lattice}$ extraction can occur away from the cluster. In this way, once a hole has nucleated, the step edge recedes from the cluster with time, leaving the cluster in

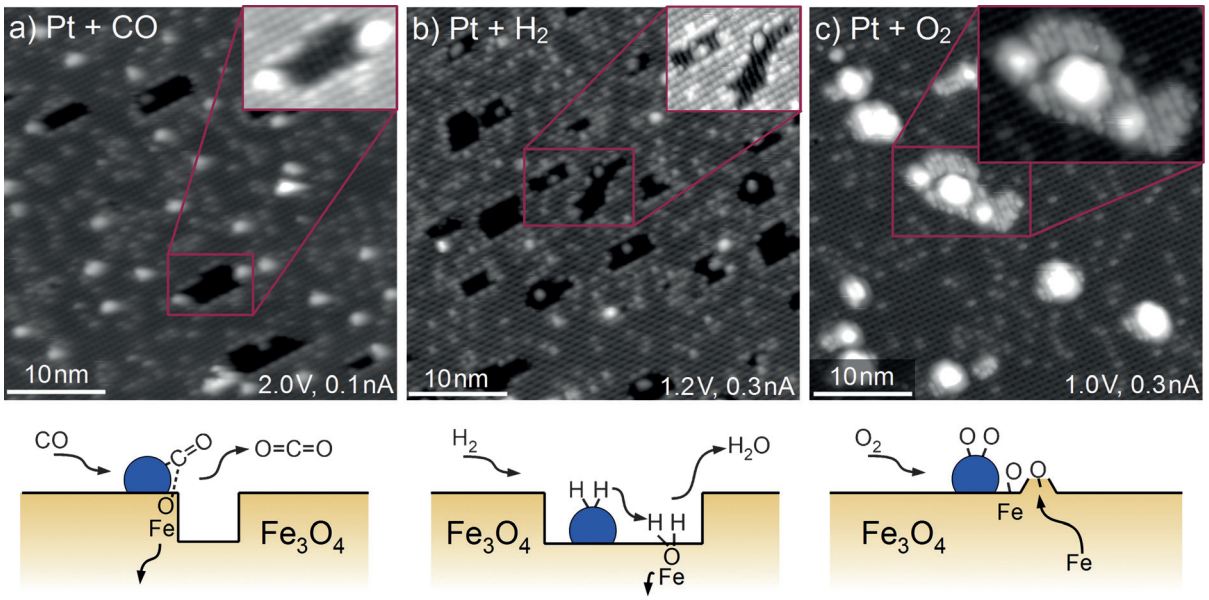

Figure 2. STM images acquired following exposure of the $Pt/Fe_3O_4(001)$ model catalyst to 1×10^{-7} mbar of CO (a), H_2 (b), or O_2 (c) at 550 K. a) Following exposure to CO (60 min), approximately 50 % of the Pt clusters sit at the edge of or inside monolayer holes in the $Fe_3O_4(001)$ terrace. The rows (rotated by 90°) of the next Fe_{oct}–O layer can be seen inside the holes (inset). The illustration shows how CO extracts $O_{lattice}$ atoms from the cluster perimeter and how CO_2 desorbs from the surface. Undercoordinated Fe atoms diffuse into the Fe_3O_4 bulk. b) Following exposure to H_2 (20 min), the clusters reside inside monolayer holes in the $Fe_3O_4(001)$ terrace. Pt adatoms are observed at regular terrace sites, and the coverage of surface OH groups is increased. The illustration shows how H_2 dissociates on the Pt cluster, spills over onto the support, and reacts with $O_{lattice}$ atoms, finally leading to the desorption of molecular water. c) Following exposure to O_2 (20 min), all Pt clusters reside on top of islands with a step height of 2 Å. On the larger islands, the rows (rotated by 90°) of the next $Fe_3O_4(001)$ layer are clearly visible. The islands result from the spillover of oxygen atoms onto the Fe_3O_4 support, which react with Fe that diffuses out from the bulk.

the bottom of the hole. Such an autocatalytic reduction of iron oxide by hydroxy groups has been reported previously.[13] Interestingly, as the clusters appear to be trapped inside the holes that they create, pretreating the $Pt/Fe_3O_4(001)$ system in H_2 at 550 K could be an effective strategy to mitigate thermal sintering during CO oxidation.

When the $Pt_{1\text{-}6}/Fe_3O_4$ model catalyst was exposed to O_2 at 550 K (Figure 2c; $p_{O_2} = 1 \times 10^{-7}$ mbar, 20 min), the Pt clusters appeared atop small islands with a step height of 2 Å. The characteristic rows of $Fe_3O_4(001)$ are clearly visible on the larger islands, suggesting that the clusters catalyze the growth of a new stoichiometric $Fe_3O_4(001)$ surface. A significant reduction in the density of clusters suggests that gas-assisted sintering occurs in the O_2 atmosphere. The growth of new $Fe_3O_4(001)$ layers has been observed on the clean surface above 900 K.[14] In the present study, however, the Pt clusters catalyze the rate-limiting step, O_2 dissociation, and highly reactive atomic O species spill over onto the support where they react with Fe supplied from the bulk at 550 K. Thus, as well as providing a sink for excess Fe during reduction, the Fe_3O_4 bulk also supplies Fe for the growth of new $Fe_3O_4(001)$ surfaces during reoxidation.[14] Similar metal-activated regrowth leads to encapsulation of the metal clusters and a loss of the catalytic activity of Pt and Pd clusters on TiO_2 surfaces,[15] but our low-energy ion scattering (LEIS) measurements (Figure S4) suggest that the Pt clusters are not encapsulated by the $Fe_3O_4(001)$ islands. Zhang et al. recently observed the encapsulation of larger Pt clusters to occur above 650 K in ultrahigh vacuum.[8a]

The data in Figure 2 clearly show that the etching and regrowth of the $Fe_3O_4(001)$ support are catalyzed by Pt clusters. To test whether similar processes still occur when multiple gases are present, we heated the Pt/Fe_3O_4 model catalyst in mixtures of CO, O_2, and H_2 at 550 K. In a 1:1 mixture of CO and O_2, the changes to the support morphology are significantly smaller than with the individual reactants (Figure S5). This could be due to two effects: Either both $O_{lattice}$ extraction and island growth occur at the same time, and their effects on the morphology cancel out, or the presence of one gas blocks the activation of the other (poisoning). To investigate this, we exposed the sample to CO/O_2 mixtures of various compositions, and found that small holes began to appear for CO/O_2 ratios of 50:1, whereas for the formation of small islands, an O_2 excess of 1:5 was required. These findings suggest that the etching and regrowth processes still occur when both CO and O_2 are present in the gas phase, although we cannot exclude that direct reaction processes also take place under such conditions. Finally, exposure of the system to a 1:1 mixture of CO and H_2 for 20 min resulted in holes that extended several layers deep into the support (Figure S5). Such a roughening of the surface suggests that the addition of H_2 to the gas mixture should help activate Pt clusters for the CO oxidation reaction.

In conclusion, the holes/islands that form in CO/O_2 rich environments provide clear evidence of the reduction and oxidation of the Fe_3O_4 support being catalyzed by Pt clusters. The legacy of these reactions is strikingly clear in STM images because the Fe_3O_4 bulk provides a sink for Fe atoms, which readily diffuse to and from the surface at the reaction temperature. In general, our data provide an atomic-scale view into metal–support interactions of importance in heterogeneous catalysis.

Acknowledgements

This material is based upon work supported as part of the Centre for Atomic-Level Catalyst Design, an Energy Frontier Research Centre funded by the U.S. Department of Energy, Office of Science, Office of Basic Energy Sciences (DE-SC0001058). G.S.P. and O.G. acknowledge support from the Austrian Science Fund (P24925-N20). R.B. acknowledges a stipend from the Vienna University of Technology and the Austrian Science Fund as part of the doctoral college SOLIDS4FUN (W1243). U.D. and J.P. acknowledge support by the European Research Council (Advanced Grant "OxideSurfaces"). A.Z. acknowledges support from the European Regional Development Fund (CEITEC, CZ.1.05/1.1.00/02.0068). We thank Prof. Mao (Tulane University) for providing the synthetic Fe_3O_4 sample used in the work.

Keywords: Mars–van Krevelen mechanism · metal–support interactions · oxide surfaces · scanning probe microscopy · supported catalysts

How to cite: *Angew. Chem. Int. Ed.* **2015**, *54*, 13999–14002
Angew. Chem. **2015**, *127*, 14205–14208

[1] a) M. M. Schubert, S. Hackenberg, A. C. van Veen, M. Muhler, V. Plzak, R. J. Behm, *J. Catal.* **2001**, *197*, 113–122; b) M. Haruta, *Catal. Today* **1997**, *36*, 153–166; c) D. Widmann, Y. Liu, F. Schüth, R. J. Behm, *J. Catal.* **2010**, *276*, 292–305; d) L. Delannoy, N. Weiher, N. Tsapatsaris, A. M. Beesley, L. Nchari, S. L. M. Schroeder, C. Louis, *Top. Catal.* **2007**, *44*, 263–273; e) M. Comotti, W.-C. Li, B. Spliethoff, F. Schüth, *J. Am. Chem. Soc.* **2006**, *128*, 917–924; f) S. Arrii, F. Morfin, A. J. Renouprez, J. L. Rousset, *J. Am. Chem. Soc.* **2004**, *126*, 1199–1205; g) J.-D. Grunwaldt, M. Maciejewski, O. S. Becker, P. Fabrizioli, A. Baiker, *J. Catal.* **1999**, *186*, 458–469; h) M. Cargnello, V. V. T. Doan-Nguyen, T. R. Gordon, R. E. Diaz, E. A. Stach, R. J. Gorte, P. Fornasiero, C. B. Murray, *Science* **2013**, *341*, 771–773; i) D. Widmann, R. J. Behm, *Acc. Chem. Res.* **2014**, *47*, 740–749; j) C. S. Polster, R. Zhang, M. T. Cyb, J. T. Miller, C. D. Baertsch, *J. Catal.* **2010**, *273*, 50–58; k) P. Panagiotopoulou, D. I. Kondarides, *Catal. Today* **2006**, *112*, 49–52; l) P. Bera, K. C. Patil, V. Jayaram, G. N. Subbanna, M. S. Hegde, *J. Catal.* **2000**, *196*, 293–301.

[2] a) X. Shao, S. Prada, L. Giordano, G. Pacchioni, N. Nilius, H.-J. Freund, *Angew. Chem. Int. Ed.* **2011**, *50*, 11525–11527; *Angew. Chem.* **2011**, *123*, 11728–11731; b) G. J. Hutchings, M. S. Hall, A. F. Carley, P. Landon, B. E. Solsona, C. J. Kiely, A. Herzing, M. Makkee, J. A. Moulijn, A. Overweg, J. C. Fierro-Gonzalez, J. Guzman, B. C. Gates, *J. Catal.* **2006**, *242*, 71–81; c) B. Yoon, H. Häkkinen, U. Landman, A. S. Wörz, J.-M. Antonietti, S. Abbet, K. Judai, U. Heiz, *Science* **2005**, *307*, 403–407.

[3] a) T. Fujitani, I. Nakamura, M. Haruta, *Catal. Lett.* **2014**, *144*, 1475–1486; b) J. Saavedra, H. A. Doan, C. J. Pursell, L. C. Grabow, B. D. Chandler, *Science* **2014**, *345*, 1599–1602.

[4] R. Bliem, E. McDermott, P. Ferstl, M. Setvin, O. Gamba, J. Pavelec, M. A. Schneider, M. Schmid, U. Diebold, P. Blaha, L. Hammer, G. S. Parkinson, *Science* **2014**, *346*, 1215–1218.

[5] A. Yanase, N. Hamada, *J. Phys. Soc. Jpn.* **1999**, *68*, 1607.

[6] G. S. Parkinson, Z. Novotny, P. Jacobson, M. Schmid, U. Diebold, *J. Am. Chem. Soc.* **2011**, *133*, 12650 – 12655.
[7] G. S. Parkinson, N. Mulakaluri, Y. Losovyj, P. Jacobson, R. Pentcheva, U. Diebold, *Phys. Rev. B* **2010**, *82*, 125413.
[8] a) K. Zhang, S. Shaikhutdinov, H.-J. Freund, *ChemCatChem* **2015**, DOI: 10.1002/cctc.201500328; b) R. Bliem, R. Kosak, L. Perneczky, Z. Novotny, Z. Mao, M. Schmid, P. Blaha, U. Diebold, G. S. Parkinson, *ACS Nano* **2014**, *8*, 7531 – 7537; c) R. Bliem, J. Pavelec, O. Gamba, E. McDermott, Z. Wang, S. Gerhold, M. Wagner, J. Osiecki, K. Schulte, M. Schmid, P. Blaha, U. Diebold, G. S. Parkinson, *Phys. Rev. B* **2015**, *92*, 075440; d) Z. Novotný, G. Argentero, Z. Wang, M. Schmid, U. Diebold, G. S. Parkinson, *Phys. Rev. Lett.* **2012**, *108*, 216103; e) Z. Novotny, N. Mulakaluri, Z. Edes, M. Schmid, R. Pentcheva, U. Diebold, G. S. Parkinson, *Phys. Rev. B* **2013**, *87*, 195410; f) G. S. Parkinson, Z. Novotny, G. Argentero, M. Schmid, J. Pavelec, R. Kosak, P. Blaha, U. Diebold, *Nat. Mater.* **2013**, *12*, 724 – 728; g) G. S. Parkinson, Z. Novotny, P. Jacobson, M. Schmid, U. Diebold, *Surf. Sci.* **2011**, *605*, L42.
[9] W. K. Jozwiak, E. Kaczmarek, T. P. Maniecki, W. Ignaczak, W. Maniukiewicz, *Appl. Catal. A* **2007**, *326*, 17 – 27.
[10] H. Y. Kim, G. Henkelman, *J. Phys. Chem. Lett.* **2013**, *4*, 216 – 221.
[11] S. Aggarwal, R. Dieckmann, *Phys. Chem. Miner.* **2002**, *29*, 695 – 706.
[12] C. H. F. Peden, G. S. Herman, I. Z. Ismagilov, B. D. Kay, M. A. Henderson, Y.-J. Kim, S. A. Chambers, *Catal. Today* **1999**, *51*, 513 – 519.
[13] W. Huang, W. Ranke, *Surf. Sci.* **2006**, *600*, 793 – 802.
[14] S. Nie, E. Starodub, M. Monti, D. A. Siegel, L. Vergara, F. El Gabaly, N. C. Bartelt, J. de La Figuera, K. F. McCarty, *J. Am. Chem. Soc.* **2013**, *135*, 10091 – 10098.
[15] a) S. Bonanni, K. Aït-Mansour, W. Harbich, H. Brune, *J. Am. Chem. Soc.* **2012**, *134*, 3445 – 3450; b) R. A. Bennett, P. Stone, M. Bowker, *Catal. Lett.* **1999**, *59*, 99 – 105.

Received: August 7, 2015
Published online: September 10, 2015

